Modal Analysis of SPRITE Noise Spectra

Frank J. Effenberger and Glenn D. Boreman

Center for Research and Education in Optics and Lasers
Department of Electrical and Computer Engineering
University of Central Florida
Orlando, FL 32816

ABSTRACT

The detector noise is the key limit to any imaging system. The unique design of Signal PRocessing In The Element (SPRITE) detectors provides measurable signal to noise improvement over ordinary detectors. The analysis and description of the noise in this type of detector is complicated by the fact that transport phenomena filter the noise spectra prior to readout. Previous analyses of the noise behavior used an approximate solution to the charge transport problem to produce expressions for the noise PSD, and yield predictions of a flat PSD at low frequencies. Measurements of real devices show a large 1/f behavior at low frequencies, but this has always been attributed to contact effects. In this paper, we use the results of the eigenmode solution to the transport problem to derive the PSD of the noise. We show that this analysis produces noise PSD's that have a 1/f dependence caused simply by the operation of the transport processes. The result is then coordinated with the similarly obtained signal response MTF to produce the frequency dependent signal to noise ratio. These are computed over several ranges of detector parameters with the intent of revealing their optimum values.

Key Words: SPRITE, infrared detectors, charge transport, noise power-spectral density.

1. INTRODUCTION

In any detector system, the fundamental limitation on total performance is the noise generated in the detector itself. For this reason, a complete description of the noise intrinsic to the detector is essential for predicting system capabilities. Noise, being a stochastic process, can have many properties that influence its behavior. In most cases, the noise in detectors can be considered a wide-sense stationary, ergodic process. When this is true, the noise can be can be described adequately by an average value and an autocorrelation function, or conversely, a power spectral density (PSD). If the PSD is known, a host of useful performance criteria, such as signal-to-noise ratio (SNR), noise-equivalent power (NEP), and detectivity (D*) can be computed. Thus, accurate determination of the noise PSD is an important step in device characterization.

SPRITE detectors[1,2] improve the signal-to-noise ratio over simpler photoconductive detectors by implementing a time-delay-and-integration (TDI) process internal to the detector element. Drift transport of carriers through the detector, in conjunction with a scanned input image, causes this to occur. Unfortunately, recombination and diffusion degrade detector performance by removing and spreading the detected charge, respectively. These imperfections affect not only the signal but also the noise generated in the detector. Thus, to understand the noise output of a SPRITE, a correct analysis of the charge transport is necessary.

In previous analyses,[3,4,5] a one-dimensional Green's function was taken as the solution to the transport equation. This solution includes diffusion, which tends to smooth the charge distribution; drift, which moves the charge along the length of the device; and recombination, which reduces the signal level over time. This solution, which describes the charge distribution resulting from a point source, is used as the basis of calculations to compute the transfer of a scanned incident-radiation distribution on the SPRITE detector bar into output as seen at the readout terminals.

To derive an expression for the noise PSD, the Green's function is used to derive the response at the readout resulting from a point source at an arbitrary position on the detector. Then, using the assumption that noise generation in the detector material is uncorrelated from point to point and time to time, the total noise spectrum is found by integrating the squared

magnitude of the point response over the entire length of the detector. This gives a result that resembles a simple low-pass-filter characteristic, with a flat power density at zero frequency and a gradual roll-off at higher frequencies.

This theory does not give complete agreement with the measurements of real devices.[6] The theory provides only qualitative description of the signal-to-noise improvement caused by the TDI function intrinsic to the SPRITE detector. Of particular interest is the behavior of actual devices at low frequencies. As mentioned before, the Green's function analysis predicts a flat PSD at low frequencies. What is actually observed is a substantial 1/f behavior.[7] While this behavior may be caused by a number of effects, such as poor contacts or thermal fluctuations, no attempt has been made to theoretically quantify or truly describe this 1/f PSD characteristic.

As discussed in our previous paper,[8] a novel method for analyzing the transport in SPRITEs was developed using a modal decomposition of the carrier density in the detector structure. This analysis is more complete than the Green's function method in that both the three-dimensional nature of the SPRITE is addressed, as well as the effect of arbitrary boundary conditions. The method of separation of variables followed by the determination of eigenmodes was used to generate the set of charge-density modes allowed in the detector. These were then used to decompose an impulsive scanned input, and then to reconstruct the resultant output.

In this paper, we shall use the same modal analysis as the basis for a study of the noise spectrum. In the next section, a short review of the assumptions and key results from the previous paper will be made. Then, using these results, an expression for the PSD of the noise will be derived. Following this, we shall compute and discuss this result. The PSD and the modulation-transfer-function (MTF) results will then be combined to produce the frequency-dependent SNR. Finally, the SNR curves will used as a means of comparison to optimize several detector parameters.

2. THE NOISE TRANSPORT PROBLEM

SPRITE detectors are complex devices having many features that are not easily analyzed. While a complete model containing all these factors would require numerical solution,[9] self-consistent models that can be solved analytically and yet still contain the main features are possible. In our previous paper, such a mathematical description of the SPRITE transport problem was given.[8] For brevity, we shall not reproduce that derivation here. All of the terminology of the model, including all of the mathematical symbology, shall be used as defined in that paper.

In the model, several assumptions concerning the physics of the charge transport are made. First, the drift-diffusion transport equation is used, assuming that the carriers are at thermal equilibrium. Second, it is assumed that the electric field in the device is a constant, which implies that the bias-induced field is stronger than any other. Third, the boundaries are described by carrier velocities, which implies that the surfaces have constant recombination rates.

To derive the noise PSD, some assumptions about the noise sources must be made. The first assumption is that the noise can be described as a random charge input at every point in the detector. It is assumed that this random signal is uncorrelated from point to point and from time to time. This implies that the PSD of this generation signal contains all frequencies (white noise), and that the signals from two different points in the detector will add in quadrature. These assumptions were used by Shepherd and Day,[3,4] and are generally applicable to SPRITE detectors. It should be noted, however, that the noise *input* being uncorrelated in space does not imply that the noise *charge* will be uncorrelated in space. The noise input is filtered by the processes of drift and diffusion to result in the noise charge distribution.[10] As will be seen in the following section, the consequence of this processing is that the PSD of the noise is no longer white.

It is also assumed in part of the derivation that the local spatial intensity of the noise is constant over the detector. Clearly, if we assume that the dominant noise source is generation-recombination noise, then the noise charge intensity will depend on the minority carrier densities. This density does not remain constant over the length of the detector because of carrier drift. Indeed, this nonuniformity in carrier density over length is the cause of variation in drift speed along the bar because of background integration.

A crude estimate of the nonuniformity of the noise can be found fairly easily if we assume that the excess carriers are only drifting, and not diffusing or interacting with the boundaries. This assumption implies that the time, t_B, a given

population of carriers, $\rho(z_B, t_B)$, has been in the SPRITE is directly proportional to the distance from the beginning of the bar, z_B. Thus we can write: $t_B = z_B / V$, where V is the drift velocity. Because no diffusion or boundary conditions exist, the population at any place and time does not interact with the neighboring populations. Thus, we can describe the excess carrier population with a simple, spatially independent generation-recombination equation, such as

$$\frac{d\rho}{dt_B} = G - \frac{\rho}{\tau}. \tag{1}$$

This has the solution,

$$\rho(z_B, t_B) = 1 - \exp\left(-\frac{t_B}{\tau}\right) = 1 - \exp\left(-\frac{z_B}{V\tau}\right). \tag{2}$$

The noise power from either generation or recombination is proportional to the rate at which these processes occur. The generation rate is a constant, G, and so the generation noise is constant. The recombination rate is equal to $\rho(z_B)/\tau$, which is not constant over the length. These two noise powers add independently, and thus give the following charge noise amplitude, $\sigma_N(z_B)$:

$$\sigma_N(z_B) = \sqrt{2 - \exp\left(-\frac{z_B}{V\tau}\right)}. \tag{3}$$

A graph of $\rho(z_B)$ and $\sigma_N(z_B)$ is given in Fig. 1, where it can be seen that the variation in noise intensity is rather small, and has a total swing of only 30% of its maximum level. For this reason, the assumption of constant intensity is made. This is not required for the following analysis to be valid. However, it does simplify the calculation and it is sufficient to produce a reasonable estimate of the frequency dependence of the noise.
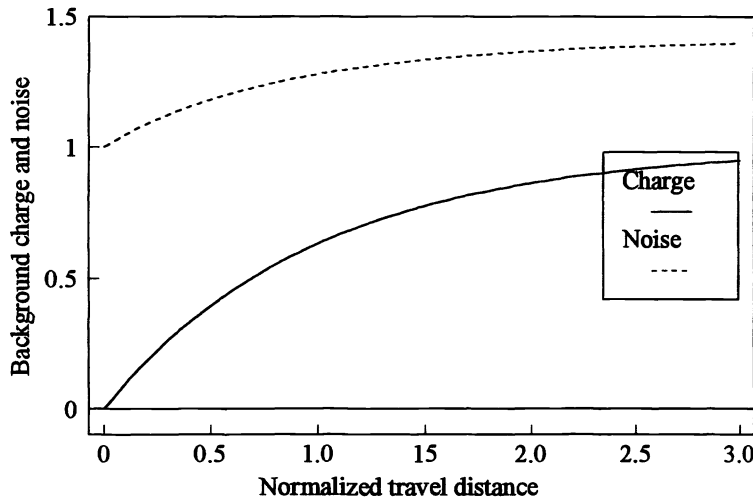
Fig. 1. Background-illumination-induced charge and resulting noise distribution in a SPRITE detector as a function of distance from the beginning of integration region.

3. NOISE POWER-SPECTRAL DENSITY (PSD)

Given the above assumptions and results, we can now derive the noise PSD of a SPRITE at its output terminals. The PSD is pivotal to characterization of the noise in that it allows computation of noise power for any given frequency band of interest. In this section, we shall begin by computing the response to a point-impulse input.

An input impulse point charge source located at a point (x'_0, y'_0, z'_0), occurring at zero time, with a strength f, denoted $q(x', y', z', t')$ can be written

$$q_i(x', y', z', t') = \delta(x' - x'_0)\,\delta(y' - y'_0)\,\delta(z' - z'_0)\,\delta(t')\,f(x'_0, y'_0, z'_0) . \tag{4}$$

Here we have allowed the strength of the point source to vary from point to point. We first must decompose this point impulse input into the modes of the structure,

$$q_i(x', y', z', t') = \sum_{p,q,r} c_{pqr}\, X_p(x')\,Y(y')\,Z(z')\,T(t')\exp(N_{dz}z') . \tag{5}$$

We can find the modal amplitudes, c_{pqr}, by using the property that the solutions are orthogonal when integrated over the domain of the detector, yielding

$$c_{pqr} = \frac{\iiint dx'\,dy'\,dz'\, X_p(x')\,Y_q(y')\,Z_r(z')\exp(-N_{dz}z')\,q_i(x', y', z', t')}{\iiint dx'\,dy'\,dz'\, X_p^2(x')\,Y_q^2(y')\,Z_r^2(z')} . \tag{6}$$

Performing the indicated integrations, we arrive at

$$c_{pqr} = \frac{\cos\!\left(k_{xp}x'_0 + p\frac{\pi}{2}\right)\cos\!\left(k_{yq}y'_0 + q\frac{\pi}{2}\right)e^{-N_{dz}z'_0}\cos\!\left(k_{zr}z'_0 + r\frac{\pi}{2}\right)}{\left[1 + \left|\mathrm{sinc}(2k_{xp})\right|\right]\left[\left[1 + \left|\mathrm{sinc}(2k_{yq})\right|\right]\right]\ \left[1 + \left|\mathrm{sinc}(2k_{zr})\right|\right]}f(x'_0, y'_0, z'_0). \tag{7}$$

We now take the modal amplitudes and compute what the output, $Q(t', x_0, y_0, z_0)$, the readout charge, will be. We can use the same mode-to-output constants, b_{pqr}, derived for the MTF calculation (Eq. 21, Ref. 8) to write

$$Q(t', x'_0, y'_0, z'_0) = \sum_{p,q,r} c_{pqr}\, u(t')\exp\!\left(-k_{pqr}^2 t'\right) b_{pqr} . \tag{8}$$

The output spectrum is found by taking the Fourier transform of this impulse response

$$\overline{Q}(\omega', x'_0, y'_0, z'_0) = \Im\{Q\} = \sum_{p,q,r} c_{pqr}\, b_{pqr}\,\frac{1}{k_{pqr}^2 + j\omega'} . \tag{9}$$

This transform of the impulse response is also the point transfer function of the SPRITE.

Now, we can relate this point transfer function to the total PSD using the assumption that the SPRITE transport process is linear. Thus, the PSD of the output due to noise at point (x'_0, y'_0, z'_0), PSD_{OUT}, is related to the input PSD of the noise at that point, PSD_{IN}, by the squared magnitude of the transfer function, thus

$$PSD_{OUT}(\omega', x'_0, y'_0, z'_0) = \overline{Q}^*(\omega', x'_0, y'_0, z'_0)\,\overline{Q}(\omega', x'_0, y'_0, z'_0)\,PSD_{IN}(\omega', x'_0, y'_0, z'_0). \tag{10}$$

Substituting the previous expression for the transfer function, we obtain the following six-dimensional sum for the output PSD resulting from a noise input at (x'_0, y'_0, z'_0),

$$PSD_{OUT}(\omega', x'_0, y'_0, z'_0) = PSD_{IN}(\omega', x'_0, y'_0, z'_0)\sum_{p,q,r}\sum_{\alpha,\beta,\gamma}\frac{b_{pqr}\,b_{\alpha\beta\gamma}\,c_{pqr}\,c_{\alpha\beta\gamma}}{\left[k_{pqr}^2 + j\omega\right]\left[k_{\alpha\beta\gamma}^2 - j\omega\right]} . \tag{11}$$

To obtain the total PSD, S_N, resulting from noise over the entire detector, we sum the contributions of each point. To do this, we must use the assumption that the noise inputs are uncorrelated from point to point in the detector. Because of this, the noise amplitudes add in quadrature, and therefore the power spectral densities add arithmetically. Since our noise inputs are infinitesimal, this requires integration over the entire detector. At this point, we use the assumption that the noise source is of constant power over the entire detector. Doing so, and using the orthogonal properties of the eigenmodes, we can obtain the following expression for the PSD of the detector

$$S_N(\omega') = \sum_{p,q,r,\gamma}\frac{b_{pqr}\,b_{pq\gamma}\,a_{r\gamma}}{\left[1 + \left|\mathrm{sinc}(2k_{xp})\right|\right]\left[1 + \left|\mathrm{sinc}(2k_{yq})\right|\right]\left[k_{pqr}^2 + j\omega\right]\left[k_{pq\gamma}^2 - j\omega\right]} . \tag{12}$$

We have defined a new set of constants, $a_{r\gamma}$, according to,

$$a_{r\gamma} = \frac{\text{Re}\left\{\exp\left[j\frac{\pi}{2}(r+\gamma)\right]\text{sinc}\left[k_{zr}+k_{z\gamma}+2jN_{dz}\right]+\exp\left[j\frac{\pi}{2}(r-\gamma)\right]\text{sinc}\left[k_{zr}-k_{z\gamma}+2jN_{dz}\right]\right\}}{\left[1+\left|\text{sinc}\left(2k_{zr}\right)\right|\right]\left[1+\left|\text{sinc}\left(2k_{z\gamma}\right)\right|\right]}. \tag{13}$$

Because the sum is symmetric with respect to r and γ, we can add each nondiagonal term, (r,γ), with its complement, (γ,r). Inspection will reveal that these terms are complex conjugates, and all the imaginary parts cancel, leaving

$$S_N(\omega') = \sum_{\substack{p,q,r,\gamma \\ \gamma \le r}} \frac{b_{pqr}b_{pq\gamma}a_{r\gamma}\left[1+\delta(r-\gamma)\right]\left[k^2_{pqr}k^2_{pq\gamma}+\omega^2\right]}{\left[1+\left|\text{sinc}\left(2k_{xp}\right)\right|\right]\left[1+\left|\text{sinc}\left(2k_{yq}\right)\right|\right]\left\{\left[k^2_{pqr}k^2_{pq\gamma}+\omega^2\right]^2+\left[k^2_{pqr}-k^2_{pq\gamma}\right]^2\omega^2\right\}}, \tag{14}$$

where the delta here signifies the kronecker delta, which is used to account for the diagonal terms $(r = \gamma)$ not having complements. This is the main result of this section.

Just as the MTF found by the modal analysis was an infinite sum, so is the PSD. The same considerations as in Ref. 8 concerning accuracy apply here as well: there is computational error, but it can be reduced to an arbitrary level. Our studies showed that the x and y summations converge to less than 0.1% error in approximately 10 terms, because of the sinc^2 dependence. The z summation convergence is slower, being driven by the modal wavenumber terms, k^2_{pqr}, in the denominator. We find that, in order to achieve an accuracy of 1%, we must include terms with r index up to 1500. While this is less than that required for the MTF calculations, this still involves a fair amount of computation. Because the z sum is two dimensional, running r to 1500 requires over 840 million terms to be computed.

4. RESULTS AND DISCUSSION

The result of section 3 was evaluated using a computer program. We used a Microsoft FORTRAN compiler on a 486DX2/66 desktop computer. This sum shares the oscillatory nature of the MTF calculation[8] and there are many more terms involved, so round off is a serious consideration. The accuracy of the sum was preserved using double-precision computations, and by evaluating and then summing the terms in an order that tended to keep major cancellation out of the final sum. Approximately one hour was required to generate a noise PSD curve on this system.
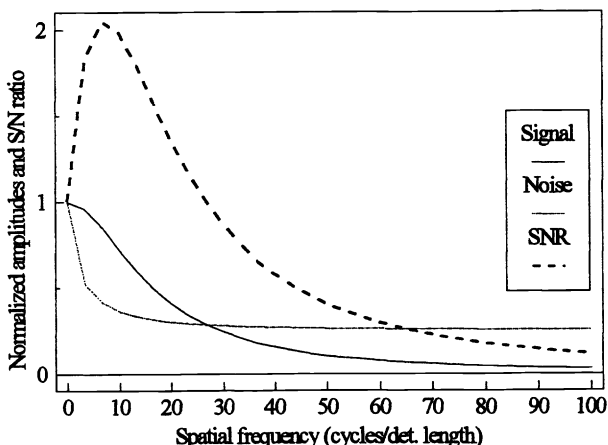
Fig. 2. Computed signal and noise amplitudes and the resulting SNR for a typical detector using eigenmode method.
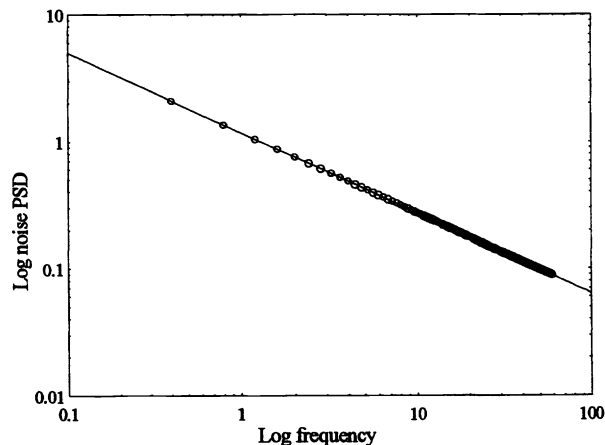
Fig. 3. Detailed graph of low-frequency behavior of the modal PSD, plotted on log-log axes. The slope of the fitted line is -0.63.

In Fig. 2, we have plotted the noise amplitude spectral density (ASD) for a typical SPRITE detector[8] along with the signal spectrum for the same detector, and their ratio. The ASD is simply the square root of the PSD, and is used here because it is directly comparable to MTF, and because experimental results are usually given in terms of ASD (i.e., $V/\sqrt{Hz}$). The noise ASD has been normalized to one at zero frequency. The most interesting feature here is the increase of the noise density at low frequencies. This strongly resembles the observed 1/f-like behavior of real devices. It is surprising that this is predicted by the modal analysis, because none of the usual phenomena associated with 1/f noise have been included in the model. This nonuniform frequency distribution results from the transport of charge alone. As the frequency increases, the noise ASD drops by a fairly large factor, finally reaching a constant high-frequency value.

By dividing the signal by the noise, we obtain the frequency-dependent signal-to-noise ratio (SNR), which has the property that the maximum SNR occurs not at zero but at some higher frequency. This helps to explain the success of various attempts at using peaking, or boost, filters to flatten the response of SPRITE detectors.[11,12] In classical scanned-detector-systems, large boost gains tend to amplify the noise present, typically resulting in poor performance. In SPRITEs, however, the SNR at the detector is high over a wide range of frequencies. Thus, the signal can be boosted at high frequencies because the noise is naturally suppressed.

A more careful analysis of the 1/f noise behavior reveals the functional dependence on frequency. A higher resolution, log-log graph of the PSD at low frequency is shown in Fig. 3. The points indicate the values computed from the modal analysis, and the line represents a curve fit of the form $y \propto x^n$. The best fit was obtained with a exponent value of -0.63. Measurements of the 1/f response of actual detectors yield a wide range of behaviors; however, the best detectors have a functional exponent dependence of -0.78.[13]

The effect of the contact boundary conditions can be seen in the next two figures. Figure 4 shows the noise ASD for a SPRITE where the contact boundary number has been varied from 0.01 to 100 time normal value. While all the curves are similar, there are two important details. The first feature is that the zero-frequency noise power is slightly elevated for contact numbers around ten. The zero-frequency power drops off on either side of this maximum, but only by 25 percent. The second feature concerns the high frequency limit of the PSD, which also has a maximum around ten. For contact numbers below ten, the PSD approaches a value approximately five times less than its peak value. For contact numbers above ten, the PSD approaches a much smaller fraction of the peak value. Even with these two factors at work, the noise is fairly independent of contact number.
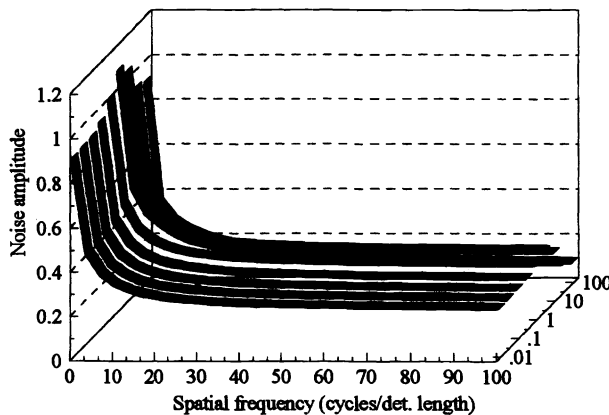
Fig. 4. Noise amplitude vs frequency as detector contact number (N_{bz}) is varied from 0.01 to 100 times normal value.
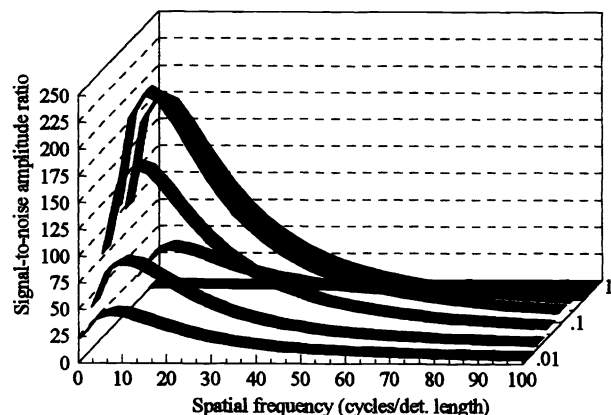
Fig. 5. Signal-to-noise ratio vs frequency as detector contact number (N_{bz}) is varied from 0.01 to 1 times nominal value.

Figure 5 shows the signal-to-noise ratios that result from combining the data in the preceding figure with SiTF data derived previously[8]. This graph tells us something that could not be determined clearly from looking at either the signal or

the noise alone. The signal analysis pointed to a contact number of one tenth the nominal, or about 0.5, as the optimum value. The noise analysis revealed that the noise is particularly high for a contact number of ten, and particularly low for high values of N_{bz}. Both these results must be combined to find the true optimum. As can be seen in Fig. 5, the optimum contact number is around 0.5. The fact that the signal varies by such large amounts, while the noise is relatively constant, makes this happen.

The most useful conclusion that we can make from this is that the contact boundary condition is very important in determining total detector performance. This is not completely surprising, as the issue has been raised for the case of simpler photoconductive detectors.[14] Because a finite optimum value of surface recombination velocity exists, then that this property must be controlled if maximum performance is to be expected. One possible method of surface velocity control would be to dope the contacting surface n^+, which causes a potential barrier that slows the recombination of minority carriers; the width and height of the barrier can be controlled in part by adjusting the penetration and concentration of the dopant. The surface velocity could also be modified through the use of different metals to fabricate the contact. In this case, the use of metals with different work functions will induce recombination barriers of differing heights, thus affecting the surface velocity. Regardless of what method is used, proper control of the contact boundaries promises large improvement in detector performance.

The effect of the top, bottom, and side boundary conditions are illustrated in the next two figures. The surfaces mentioned are nominally insulating, because any charge recombining on these surfaces is lost charge which is not read as signal. Figure 6 shows the noise ASD for a typical SPRITE as the side boundary numbers, N_{bx} and N_{by}, are varied from 0.01 to 100 times nominal value. Very little change is seen, with no change in the zero-frequency or at the high-frequency limits. A small widening of the '1/f' peak for high numbers occurs, but this effect is rather small. Figure 7 shows the SNR for this set of detectors. It can be seen that the SNR is insensitive to the side boundary conditions until they approach 100 time normal value, which corresponds to boundary numbers around unity.
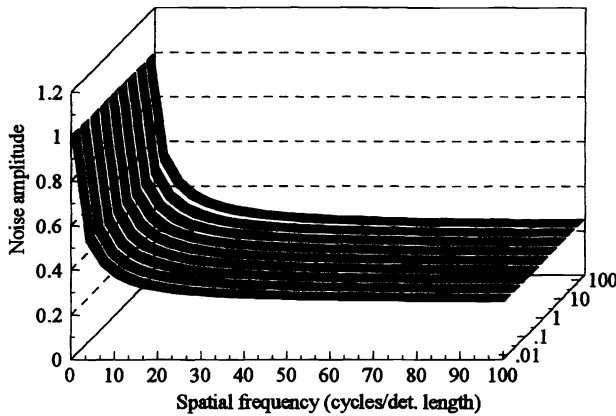
Fig. 6.Noise amplitude vs frequency as top, bottom, and side boundary numbers (N_{bx}, N_{by}) are varied from 0.01 to 100 times nominal value.
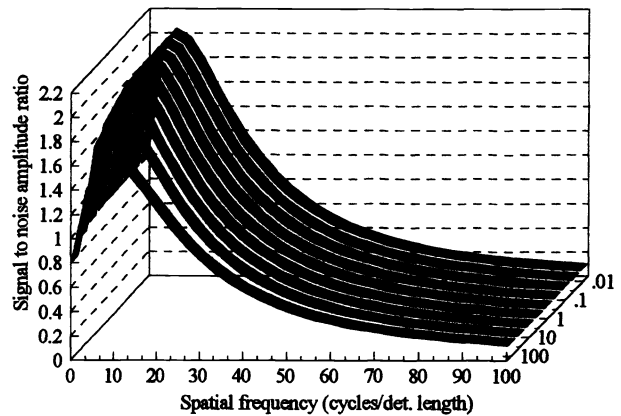
Fig. 7. Signal-to-noise ratio vs frequency as top, bottom, and side boundary numbers (N_{bx}, N_{by}) are varied from 100 to 0.01 times nominal value.

The influence of the width of the detector can be seen in Fig. 8. This shows the signal-to-noise ratio for a range of spreading number, N_{sx} from 0.01 to 100 time normal. The width spreading parameter is inversely proportional to the square of the width, and so this range corresponds to a range of widths from 0.1 to 10 times normal. The side boundary conditions were raised to be five times normal to amplify any effects of the spreading parameter. Even with this 'coaxing' of the model, no change in the noise density, signal level, and SNR was detected. This can be explained by the fact that when the boundary condition is mostly insulating, the high-order transverse modes of the structure do not contribute significantly to the output. The spreading parameter only affects the high-order modes, and thus it has little affect on the output.
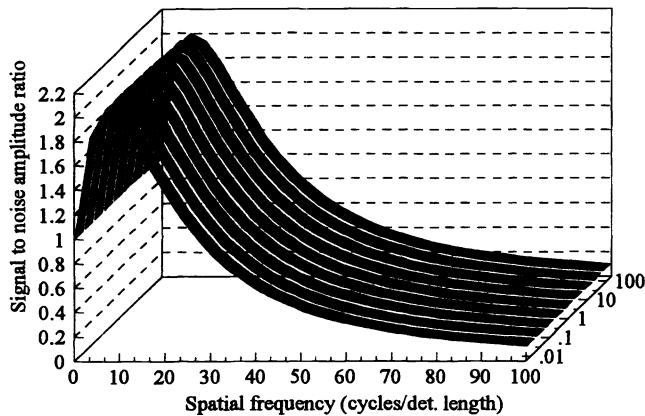
Fig. 8. Signal-to-noise ratio vs frequency as width spreading parameter (N_{sx}) is varied from 100 to 0.01 times nominal value. The side boundary number (N_{bx}) is 5 times nominal value.

There are two interrelated conclusions we can draw from these two studies of the transverse effects in SPRITEs. The first is that the top, bottom, and side boundary conditions should be made as insulating as possible, but that efforts to reduce the boundary numbers below 0.1 are unnecessary. The nominally insulating boundaries can be made even less leaky through the use of better passivation materials or the use of controlled doping, just as in the case of the contacts. The second conclusion is that, as long as the side boundaries are insulating, the width of the detector is not important in determining final detector response. This fact might offer possibilities for new detector layouts or designs, as it tends to remove one of the many considerations restricting detector design.

5. CONCLUSIONS

The detector noise of SPRITE has been analyzed using the newly developed method of modal analysis. This method differs from previous analyses in that the model on which it is based is more complete, and includes the boundary conditions and three-dimensional nature of the detector. The PSD was computed for typical detectors, and it was found to have a 1/f-like low-frequency feature, in agreement with measured spectra. The noise PSD was computed for SPRITEs with varying boundary and width parameters. These spectra were then compared with signal spectra for the same conditions. Several optimum operating points have been identified, as well as several methods of achieving them.

6. ACKNOWLEDGMENT

7. REFERENCES

1.   C. T. Elliot, US Patent #3,995,159, Nov. 30, 1976.
2.   C. T. Elliot, "New detector for thermal imaging systems," Electron. Lett. 17, 312-313 (1981).
3.   D. J. Day and T. J. Shepherd, "Transport in photoconductors - I," Solid State Electronics 25, 707-712 (1982).
4.   T. J. Shepherd and D. J. Day, "Transport in photoconductors - II," Solid State Electronics 25, 713-718 (1982).
5.   G. D. Boreman and A. E. Plogstedt, "Modulation transfer function and number of equivalent elements for SPRITE detectors," Appl. Opt., 27, 4331-4335 (1988).
6.   S. P. Braim and A. P. Campbell, "TED (SPRITE) detector MTF," IEE Conf. 228, 63-66 (1983).
7.   S.P. Braim, "The measurement and analysis of the noise frequency spectrum for SPRITE infrared detectors," Proc. SPIE 590, 164-171 (1985).
8.   F. J. Effenberger and G. D. Boreman, "Modal Analysis of SPRITE Transport Processes," OE/Aerospace Sensing and Dual Use Photonics, Proc. SPIE 2470, paper 13, (1995).

9.   T. Ashley, C. T. Eliot, and A. M. White, "Optimization of spatial resolution in SPRITE detectors," Infrared Physics **24**, 25-33 (1984).

10.   A. Van der Ziel, *Fluctuation phenomena in semi-conductors*. (Academic Press, Inc., New York, 1959) 33-36.

11.   P. Fredin, "Optimum choice of anamorphic ratio and boost filter parameters for a SPRITE based IR sensor," Proc. SPIE **1488**, 432-442 (1991).

12.   P. Fredin, G. D. Boreman, "Normalized detectivity as a function of diffusion length for SPRITE detectors," Proc. SPIE **1969**, 139-149 (1993).

13.   GEC-Marconi Infra-Red Limited, Private Communication, March 1994.

14.   A. Józwikowska, K. Józwikowski, A. Rogalski, "Performance of mercury cadmium telluride photoconductive devices," Infrared Physics 31, 543-554 (1991).